Supporting Information

Robust and efficient membrane contactor for carbon dioxide capture enabled by thin-film composite Janus membrane

Wenting Zhou[1,2], Chunlei Su (✉)[3], Dejun Feng[1,2], Yuanmiaoliang Chen[4], Liting Pan[1,2], Di He[2], Zhangxin Wang (✉)[1,2]

1 Guangdong Basic Research Center of Excellence for Ecological Security and Green Development, School of Ecology, Environment and Resources, Guangdong University of Technology, Guangzhou 510006, China
2 Key Laboratory for City Cluster Environmental Safety and Green Development of the Ministry of Education, School of Ecology, Environment and Resources, Guangdong University of Technology, Guangzhou 510006, China
3 Institute of Process Engineering, Chinese Academy of Sciences, Beijing 100190, China
4 Department of Civil and Environmental Engineering, Rice University, Houston Texas 77005, USA

✉ Corresponding authors
E-mail: suchunlei@ipe.ac.cn (C. Su); zhangxin.wang@gdut.edu.cn (Z. Wang)

1. Membrane fabrication procedures

The fabrication process for the TFC Janus membrane is schematically illustrated in Fig. S1a, while the fabrication of the monolithic PVDF membranes with varying hydrophobicities is depicted in Fig. S1b.

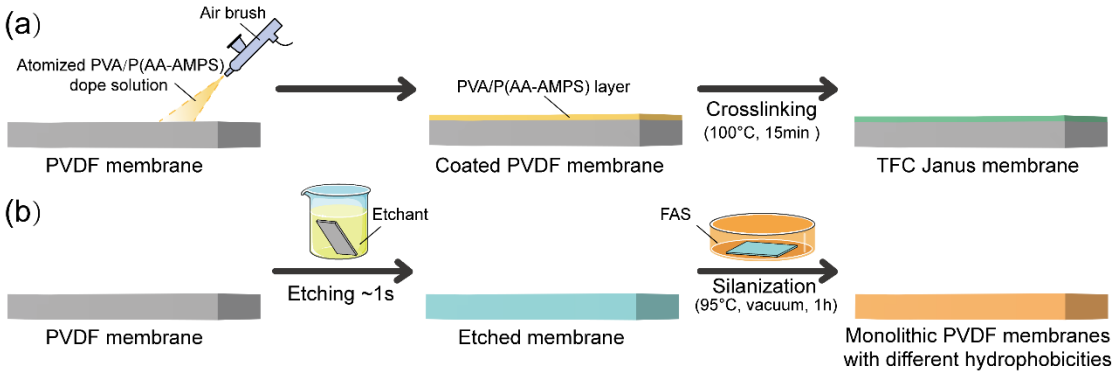

Fig. S1 Schematics illustrating the fabrication processes of (a) the TFC Janus membrane and (b) monolithic PVDF membranes with varying hydrophobicities.

2. Microstructure of the pristine PVDF membrane

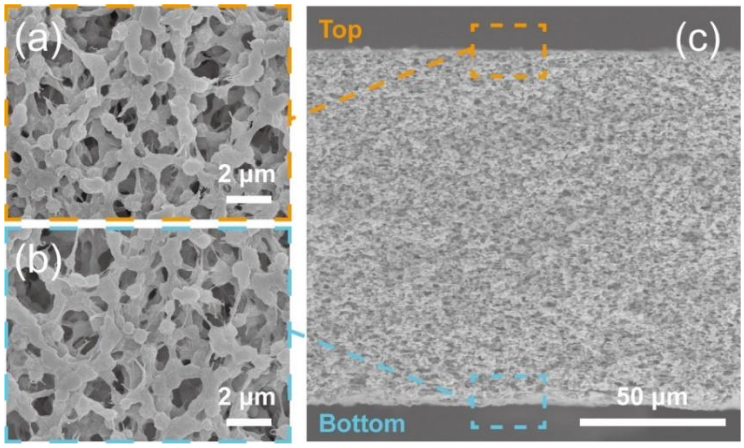

Fig. S2 SEM images of the pristine PVDF membrane: (a) top surface, (b) bottom surface, and (c) cross-section.

3. Solute filtration tests

The mean pore size and pore size distribution of the PVA surface layer on the TFC Janus membrane were determined using the experimental setup illustrated in Fig. S3.

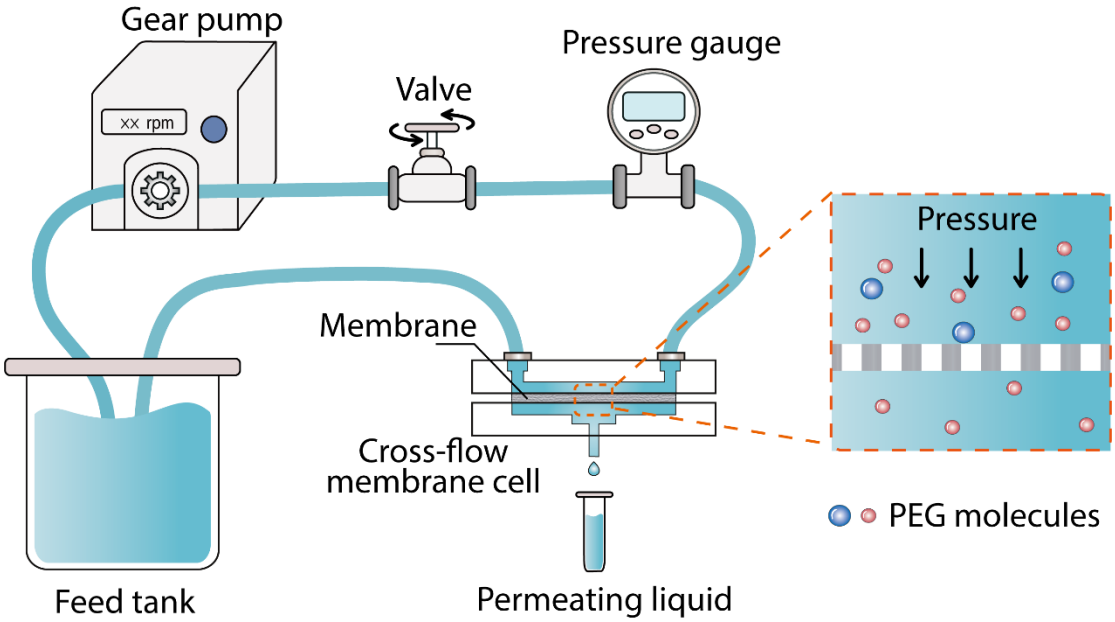

Fig. S3 Schematic diagram of the solute filtration test setup. The hydraulic pressure was controlled using a gear pump and a valve, with pressure measurements taken via a pressure gauge.

The solute filtration tests were performed with four feed solutions containing 200 ppm polyethylene glycol (PEG) with molecular weights of 400, 600, 1000, and 1500 Da. Before testing, the TFC Janus membrane was pre-wetted with ethanol and thoroughly rinsed with DI water. The membrane was then assembled into the testing cell, and the PEG solution was pumped towards the membrane under a hydraulic pressure of 6 bar.

The PEG concentration in the permeate (c_p) was measured using a total organic carbon analyzer (TOC-L, Shimadzu, Japan). Given the known feed PEG concentration ($c_f = 200$ ppm), the PEG rejection (R) was calculated as

$$R = (1 - \frac{c_p}{c_f}) \times 100\% \quad \text{(S1)}$$

The Stokes diameter of PEG (d_s) was determined based on its molecular weight (M_w),

$$d_s = 33.46 \times 10^{-12} {M_w}^{0.557} (\leq 35{,}000) \quad \text{(S2)}$$

The mean pore size (μ_s) of the PVA layer was defined as the d_s value corresponding to $R = 50\%$. The pore size distribution of the tested membrane was then calculated using the following relationship,

$$\frac{dR(d_p)}{d(d_p)} = \frac{1}{d_p \sqrt{2\pi} ln\sigma_p} exp\left[-\frac{(lnd_p - ln\sigma_p)^2}{2(ln\sigma_p)^2}\right] \quad \text{(S3)}$$

where d_p is the pore diameter, and σ_p is the geometric standard deviation, determined from the ratio of d_s values at $R = 84.13\%$ and $R = 50\%$.

4. Gas permeability measurements

We assessed the effect of the modification process on membrane structure by comparing the gas permeability of the membranes before and after modification. Gas permeability was measured using the setup illustrated in Fig. S4. A dried membrane sample with an effective area of 3 cm^2 was placed in a dead-end testing cell. A 15 vol% CO_2/N_2 gas mixture was directed into the testing cell at room temperature, with an applied pressure incrementally increased. The gas flow rate exiting the testing cell was recorded as a function of the applied pressure, allowing the gas permeability to be calculated. Each membrane underwent three independent measurements, and the averaged results with error bars were reported.

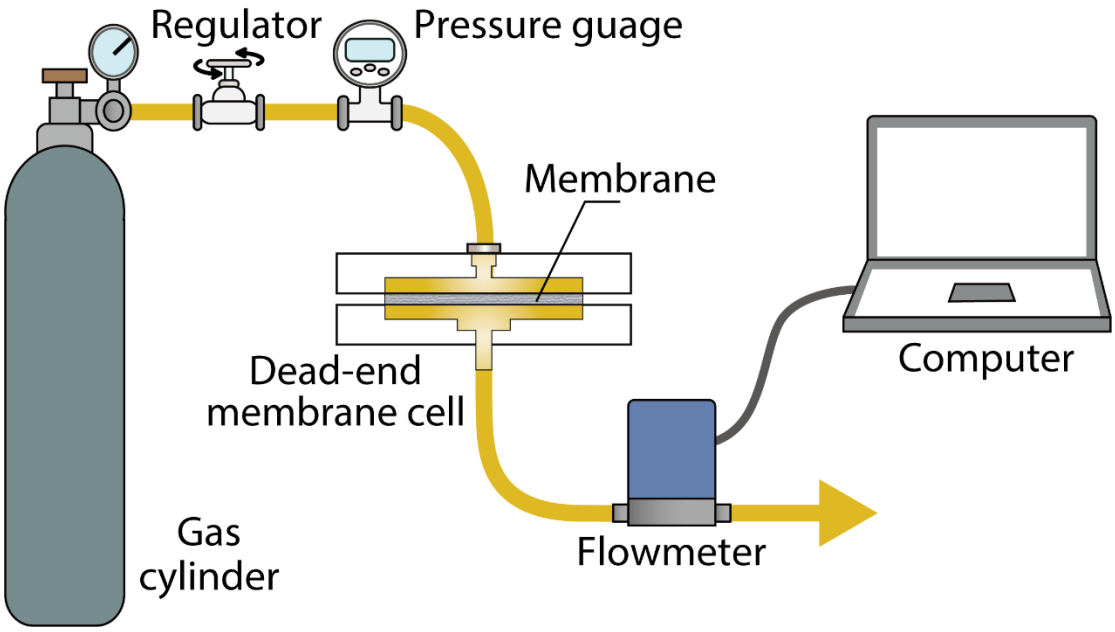

Fig. S4 Schematic diagram of the experimental setup for gas permeability measurements. The applied pressure on the gas stream was controlled using a regulator and monitored with a pressure gauge. The gas flow rate exiting the testing cell was measured with a flowmeter connected to a computer.

5. Diffusion experiments

We performed diffusion experiments to measure the MEA permeability of the monolithic PVDF membrane and the TFC Janus membrane. Prior to the experiments, a series of MEA solutions with concentrations of 0.001 mol/L, 0.01 mol/L, 0.1 mol/L, 0.5 mol/L, 1 mol/L, and 2 mol/L were prepared, and their corresponding pH values were measured using a pH meter (Thermo Scientific, Orion Star A214, USA) to establish the relationship between MEA concentration (C) and pH.

In each diffusion experiment, a small membrane coupon (1 cm^2) was pre-wetted with ethanol, rinsed with DI water, and mounted in a two-chamber diffusion cell (Fig. S5). The two chambers were filled with 5 mol/L MEA solution and DI water, respectively. The pH of the DI water chamber was continuously monitored over time, enabling the calculation of MEA concentration in that chamber. Using the time-dependent MEA concentration, the MEA permeability of the membrane was determined.

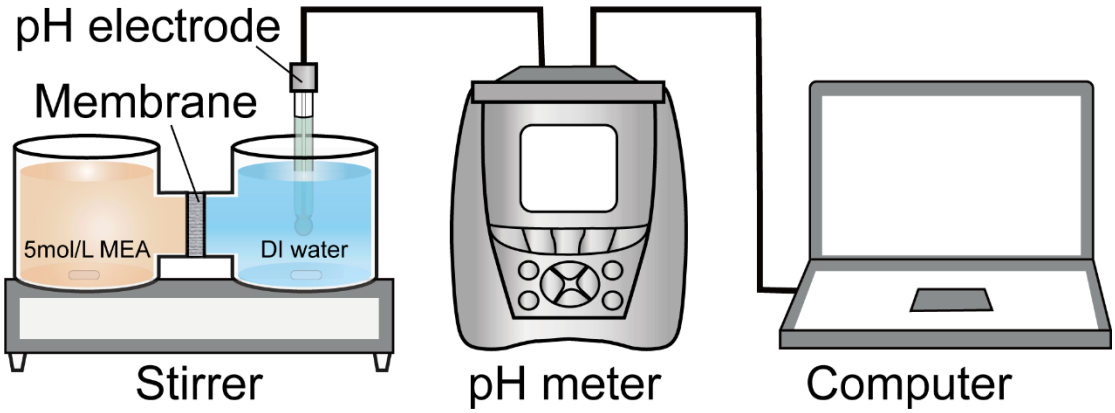

Fig. S5 Schematic diagram of the setup used in diffusion experiments.

6. Gas-Liquid membrane contactor (GLMC) experiments for CO_2 absorption

The setup for the GLMC experiments is shown in Fig. S6. At the start of each experiment, a mixed gas stream (i.e., 15 vol% CO_2/N_2) was introduced into one side of the membrane cell for 30 min to purge any air. Subsequently, the absorbent stream (1 mol/L MEA solution) was introduced into the other side of the membrane cell. The effective membrane area in the cell was 2 cm × 4 cm.

To minimize the impact of pulse flow on the results, a pulse damper was installed in the absorbent stream, and digital pressure gauges were used to monitor hydraulic pressures. The flow rate of the inlet mixed gas was maintained at 170 sccm using a gas mass flow controller (MFC, Sevenstar, D07-19, China), while the flow rate of the MEA solution was controlled at 0.3 L/min by a peristaltic pump. To prevent the formation of gas bubbles in the MEA solution, the pressure of the mixed gas was kept ~10 kPa lower than that of the MEA solution.

As the mixed gas passed through the GLMC cell, CO_2 was absorbed by the MEA solution. A gas flowmeter (GFM, Sevenstar, CS200, China) and a CO_2 analyzer (Wandi, PDA600, China) continuously monitored the flow rate of the mixed gas and the CO_2 concentration, respectively. Using the measured flow rate and CO_2 concentration data, the real-time CO_2 flux (J_{CO_2}, mol/m^2/s) in the GLMC system could be calculated,

$$J_{CO_2} = \frac{P(C_{in}Q_{in} - C_{out}Q_{out})}{A_m RT} \quad \text{(S4)}$$

where C_{in} and C_{out} are the CO_2 concentrations (vol%) at the inlet and outlet of the membrane cell, respectively, Q_{in} and Q_{out} are the volume flow rates of the mixed gas (m^3/s) at the inlet and outlet, respectively, P is the pressure of the gas mixture (atm), A_m is the effective area of the membrane (m^2), R and T are the ideal gas constant and operating temperature, respectively.

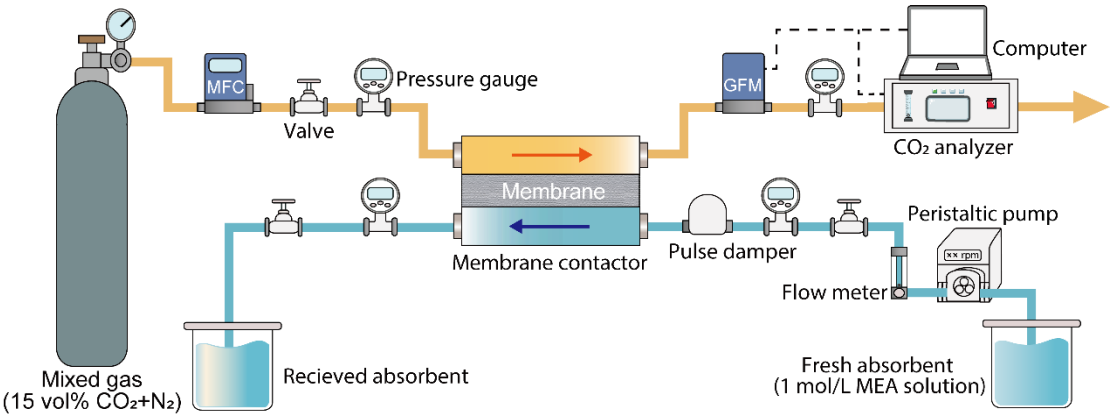

Fig. S6 Schematic diagram of the setup used for the GLMC experiment.

7. Electrochemical impedance tests

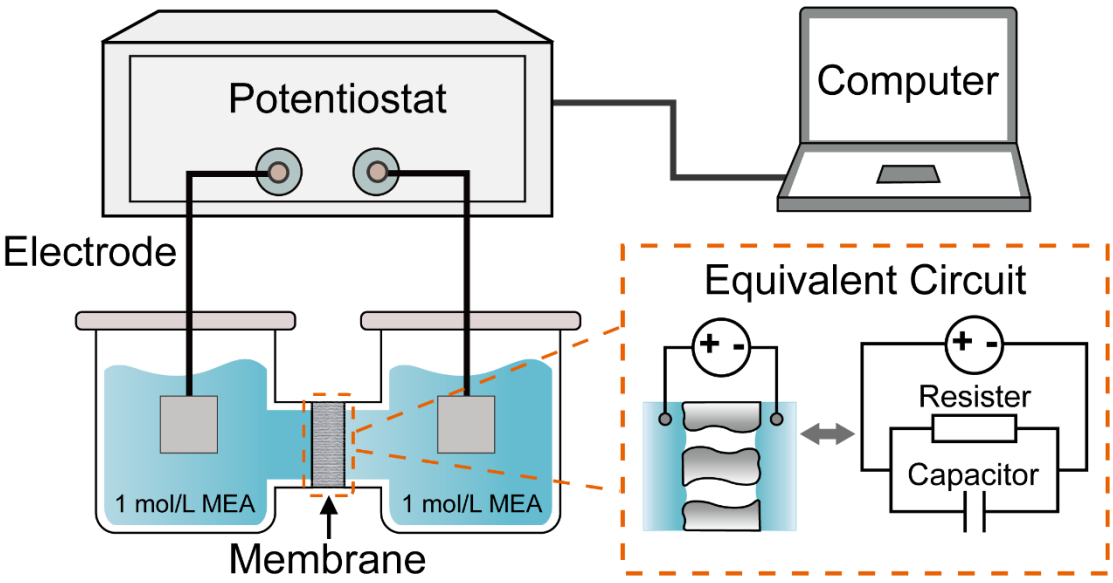

Fig. S7 Schematic diagram of the experimental setup for electrochemical impedance tests.

8. UTDR tests

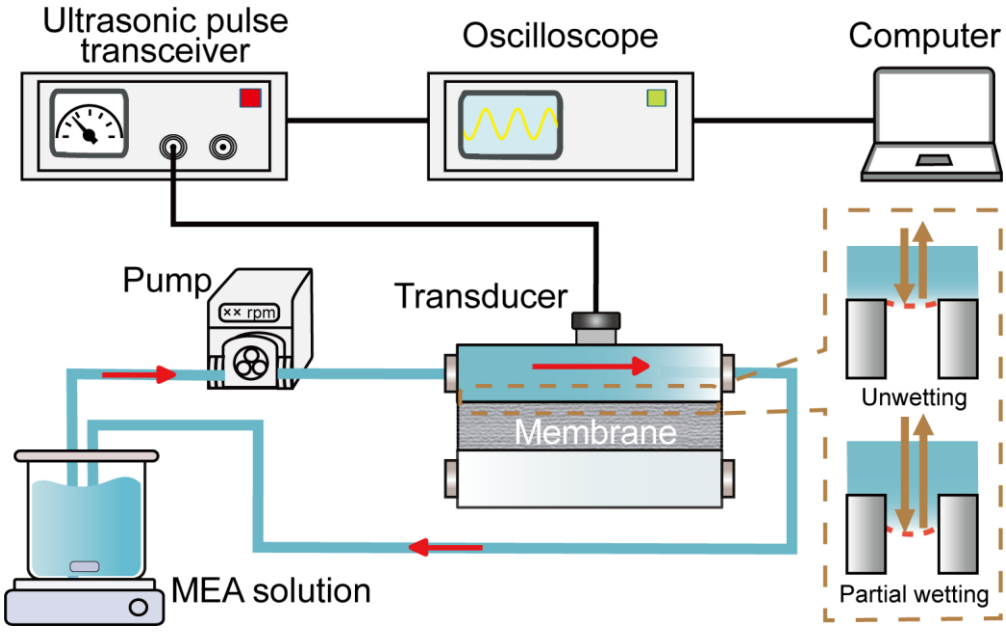

Fig. S8 Schematic diagram of the experimental setup for UTDR tests.

9. Calculation equations

The penetration depth (d_{wet}) of the MEA solution into the membrane can be calculated as (Luo et al., 2023; Wan et al., 2023),

$$d_{wet} = \frac{V\Delta t}{2} \tag{S5}$$

where V is the velocity of ultrasonic waves in the MEA solution, and Δt is the difference in arrival time obtained from UTDR tests.

The effective membrane thickness (d_{eff}) is defined as the thickness of the non-wetted portion of the membrane and is calculated as

$$d_{eff} = d_{mem} - d_{wet} \tag{S6}$$

where d_{mem} is the total membrane thickness, and d_{wet} is the penetration depth obtained from UTDR tests. For the TFC Janus membrane, d_{mem} refers to the thickness of the PVDF substrate, as the PVA layer is hydrophilic.

The air-filled hydrophobic membrane can be modeled as a capacitor, and the capacitance (C_{mem}) can be estimated (Li et al., 2020),

$$C_{mem} = \frac{\varepsilon_0 \varepsilon_m A_{eff}}{d_{eff}} \tag{S7}$$

Thus, the effective gas-liquid interface area (A_{eff}) in the membrane can be calculated,

$$A_{eff} = \frac{C_{mem} d_{eff}}{\varepsilon_0 \varepsilon_m} \tag{S8}$$

where ε_0 and ε_m are the permittivity of air (or vacuum) and the relative permittivity of the air-membrane matrix, respectively.

10. Long-term performance of the TFC Janus membrane

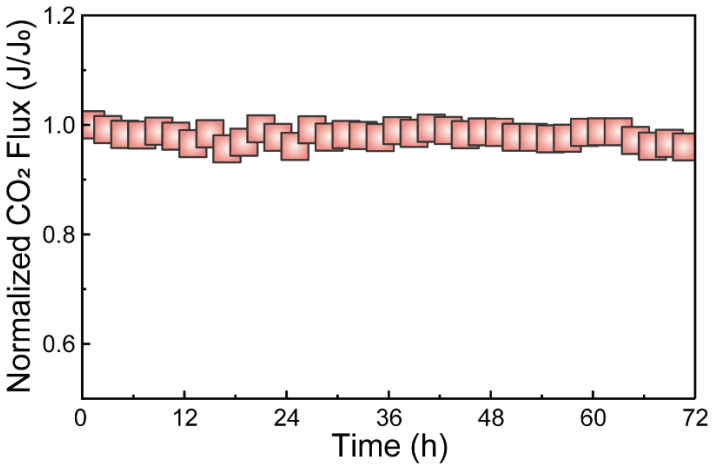

Fig. S9 Normalized CO_2 flux for the TFC Janus membrane in a 72-h GLMC experiment.

11. Comparison of the TFC Janus membrane with reported membranes

Table S1 Performance comparison of the TFC Janus membrane and representative membranes reported in the literature.

Membranes	Feed gas	Absorbent	CO_2 flux ($mol/m^2/s$)	CO_2 flux reduction	Ref.
PP	CO_2/Air (14/86)	20 wt% MEA	0.40×10^{-3}	66 h, ~ 15%	(Franco et al., 2009)
PP	CO_2/Air (15/85)	1 mol/L MEA	0.40×10^{-3}	-	(Khaisri et al., 2009)
PP	CO_2/N_2 (15/85)	1 mol/L MEA	1.70×10^{-3}	30 d, ~ 37%	(Wang et al., 2013)
PP	CO_2/N_2 (20/80)	1 mol/L MEA	0.23×10^{-3}	10 d, ~ 56%	(Lv et al., 2012)
PVDF	CO_2/Air (15/85)	1 mol/L MEA	1.46×10^{-3}	-	(Khaisri et al., 2009)
PVDF	CO_2/N_2 (15/85)	1 mol/L MEA	1.64×10^{-3}	30 d, ~ 50%	(Wang et al., 2013)
PVDF	CO_2/Air (20/80)	2 mol/L MEA	1.26×10^{-3}	-	(Rongwong et al., 2015)
PVDF	Pure CO_2	2 mol/L MEA	2.43×10^{-3}	3 d, ~ 20%	(Atchariyawut et al., 2007)
PVDF	CO_2/N_2 (9/91)	AMP + PZ	1.36×10^{-3}	2 h, ~ 90%	(Lin et al., 2016)
PVDF	CO_2/N_2 (19/81)	1 mol/L DEA	0.74×10^{-3}	-	(Gong et al., 2021)
PTFE	CO_2/Air (15/85)	1 mol/L MEA	1.82×10^{-3}	-	(Khaisri et al., 2009)
PTFE	CO_2/Air (20/80)	2 mol/L MEA	2.22×10^{-3}	-	(Rongwong et al., 2015)
PTFE	CO_2/N_2 (20/80)	30 wt% MEA	0.63×10^{-3}	-	(Bougie et al., 2014)
PTFE	CO_2/N_2 (15/85)	DMEA + PZ	1.55×10^{-3}	-	(Cao et al., 2019)
PTFE	Pure CO_2	AHPD + PZ	2.17×10^{-3}	-	(Bougie et al., 2015)
PTFE	CO_2/N_2 (9/91)	AMP + PZ	2.50×10^{-3}	16 h, ~ 93%	(Huang et al., 2018)
TFC Janus	CO_2/N_2 (15/85)	1 mol/L MEA	2.85×10^{-3}	3 d, ~ 4%	This work

Note: PP: polypropylene; PVDF: polyvinylidene fluoride; PTFE: polytetrafluoroethylene; MEA: monoethanolamine; DEA: diethanolamine; DMEA: dimethylethanolamine; PZ: piperazine; AMP: 2-amino-2-methyl-1-propanol; AHPD: 2-amino-2-hydroxymethyl-1,3-propanediol; All CO_2 flux values are unified as $mol/m^2/s$ for comparative purposes.

12. Pore size distributions of the pristine PVDF membrane

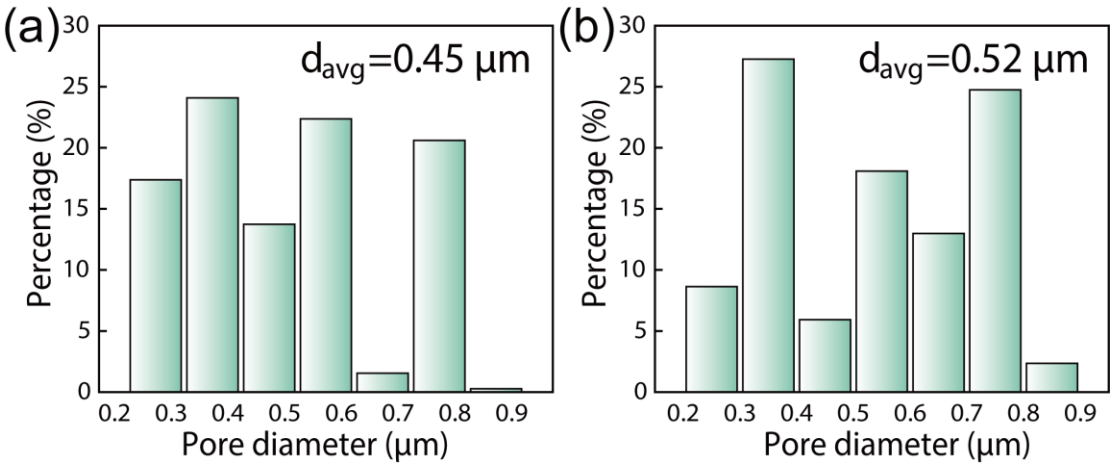

Fig. S10 Pore size distributions of the PVDF membrane (a) before and (b) after a 24-h GLMC experiment.

13. UTDR echo waveforms results

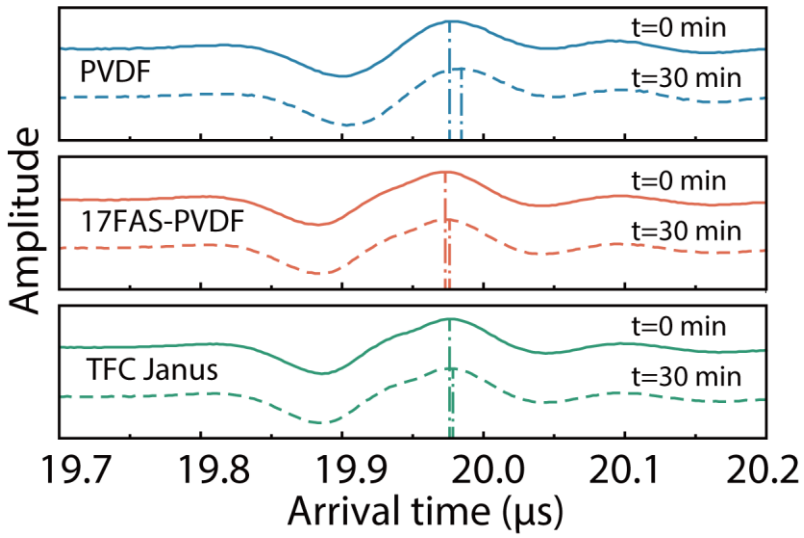

Fig. S11 UTDR echo waveforms of the pristine PVDF membrane, 17FAS-PVDF membrane, and TFC Janus membrane at t = 0 min (solid line) and t = 30 min (dashed line). In each test, a 1 mol/L MEA solution was used as the testing liquid.

References

Atchariyawut S, Jiraratananon R, Wang R (2007). Separation of CO_2 from CH_4 by using gas–liquid membrane contacting process. Journal of Membrane Science, 304(1-2): 163-172

Bougie F, Iliuta I, Iliuta M C (2014). Absorption of CO_2 by AHPD–Pz aqueous blend in PTFE hollow fiber membrane contactors. Separation and Purification Technology, 138: 84-91

Bougie F, Iliuta I, Iliuta M C (2015). Flat sheet membrane contactor (FSMC) for CO_2 separation using aqueous amine solutions. Chemical Engineering Science, 123: 255-264

Cao F, Gao H, Xiong Q, Liang Z (2019). Experimental studies on mass transfer performance for CO_2 absorption into aqueous N,N-dimethylethanolamine (DMEA) based solutions in a PTFE hollow fiber membrane contactor. International Journal of Greenhouse Gas Control, 82: 210-217

Franco J A, Demontigny D, Kentish S E, Perera J M, Stevens G W (2009). Effect of amine degradation products on the membrane gas absorption process. Chemical Engineering Science, 64(18): 4016-4023

Gong H, Pang H, Du M, Chen Z (2021). Fabrication of a superhydrophobic mixed matrix PVDF-SiO_2-HDTMS hollow fiber membrane for membrane contact carbon dioxide absorption. Cleaner Engineering and Technology, 5: 100278

Huang A, Chen L-H, Chen C-H, Tsai H-Y, Tung K-L (2018). Carbon dioxide capture using an omniphobic membrane for a gas-liquid contacting process. Journal of Membrane Science, 556: 227-237

Khaisri S, Demontigny D, Tontiwachwuthikul P, Jiraratananon R (2009). Comparing membrane resistance and absorption performance of three different membranes in a gas absorption membrane contactor. Separation and Purification Technology, 65(3): 290-297

Li C, Li X, Du X, Zhang Y, Wang W, Tong T, Kota A K, Lee J (2020). Elucidating the trade-off between membrane wetting resistance and water vapor flux in membrane distillation. Environmental Science & Technology, 54(16): 10333-10341

Lin Y-F, Ye Q, Hsu S-H, Chung T-W (2016). Reusable fluorocarbon-modified electrospun PDMS/PVDF nanofibrous membranes with excellent CO_2 absorption performance. Chemical Engineering Journal, 284: 888-895

Luo Y, Shao S, Mo J, Yang Y, Wang Z, Li X (2023). Spatio-temporal progression and influencing mechanism of local wetting in membrane distillation. Journal of Membrane Science, 670: 121374

Lv Y, Yu X, Jia J, Tu S-T, Yan J, Dahlquist E (2012). Fabrication and characterization of superhydrophobic polypropylene hollow fiber membranes for carbon dioxide absorption. Applied Energy, 90(1): 167-174

Rongwong W, Fan C, Liang Z, Rui Z, Idem R O, Tontiwachwuthikul P (2015). Investigation of the effects of operating parameters on the local mass transfer coefficient and membrane wetting in a membrane gas absorption process. Journal of Membrane Science, 490: 236-246

Wan H, Li X, Luo Y, Shi D, Gong T, An A K, Shao S (2023). Early monitoring of pore wetting in membrane distillation using ultrasonic time-domain reflectometry (UTDR). Water Research, 240: 120081

Wang L, Zhang Z, Zhao B, Zhang H, Lu X, Yang Q (2013). Effect of long-term operation on the performance of polypropylene and polyvinylidene fluoride membrane contactors for CO_2 absorption. Separation and Purification Technology, 116: 300-306